On the optical band gap in certain ternary phosphate and TeO$_2$ based glasses

H. TICHA, L. TICHY[a,*]

Faculty of Chemical Technology, University of Pardubice, 532 10 Pardubice, Czech Republic
[a]*Institute of Macromolecular Chemistry of the Academy of Sciences of the Czech Republic v.v.i., Heyrovsky sq. 2,120 06 Prague, Czech Republic*
[*]*Present address: Joint Laboratory of Solid State Chemistry of Institute of Macromolecular Chemistry of the Academy of Sciences of the Czech Republic v.v.i. and the University of Pardubice, 532 10 Pardubice, Czech Republic*

An emphasis is placed on the fact that the correct determination of the optical band gap using the Tauc or Davis- Mott model requires the use of the correct samples thickness for the optical transmission measurements. For 46 heavy metal oxide glasses based on P$_2$O$_5$ or TeO$_2$ the optical band gap values were determined using the Davis – Mott model from the classical optical absorption measurements on the samples with the thickness varying from 0.5 to 4 μm. For PbO-ZnO-P$_2$O$_5$ glasses and for heavy metal oxide glasses based on TeO$_2$ the band gaps in the regions 4.6-5.39 eV and 3.14-3.61 eV, respectively, were found. Using the simplest version of the alloying model the band gaps for glasses PbO-ZnO-P$_2$O$_5$ in the region 4.11-5.78 eV and for heavy metal oxide glasses based on TeO$_2$ in the region 3.02-3.75 eV were calculated.

1. Introduction

Recently, considerable attention has been given to the preparation and study of the physical properties of various ternary glasses based on heavy metal oxides (HMO). These are typically represented by glasses which mainly include a high content of PbO, Bi$_2$O$_3$ often in combination with other HMO such as WO$_3$, Nb$_2$O$_5$, TeO$_2$ [1]. Commonly, the optical band gap (E$_g$) values are determined as a key characteristic of a semiconductor and glass. We, however, found that quite often in recent years published band gap values were lower than those we determined for very similar or even for the same glasses [2-4]. The optical band gap (E$_g$) limits the optical transmission in the short wavelength absorption region of a material. Via various relations E$_g$ is related to the other most important quantity of any optical material namely to the linear refractive index (n) [5-8] and the non-linear refractive index (n$_2$) [9-12]. As emphasized by Tanaka [13] "...the optical band gap is the decisive parameter determining nonlinear optical properties of noncrystalline solids". Hence it is important to know the correct band gap values and to determine the origin of the disagreement in the band gap values. We are convinced that there are two possible origins which could be responsible for reducing the band gap values of ternary glasses based on HMO. The first origin is glass darkening associated in all probability with the thermal decomposition of certain oxides namely Bi$_2$O$_3$ and TeO$_2$ if too high synthesis temperatures are used and/or inconvenient crucible is used for the glass melting [14]. The second origin of the band gap reduction is the incorrect application of the Tauc model [15] or the Davis-Mott model [16] for determination of the optical band gap in amorphous solids.

The aim of this paper is to (i) briefly recapitulate certain facts related to the correct determination of E$_g$ in the glasses from the classical optical transmission measurements and (ii) summarize the optical band gap values for 46 different glasses based on HMO we determined using the Davis-Mott model.

2. Recapitulation

The typical short wavelength absorption edge (SWAE) for many glasses or amorphous semiconductors is shown in Fig. 1. For the purposes of this paper we shall consider only parts A and B. In the high absorption region (A) where α > 10^3 – 10^4 cm^{-1} the absorption coefficient (α) is expressed by the following relation [17]:

$$\alpha = [2(\pi e P/m)^2\, V_{cell}/c\omega n] \int g_i(E)g_f(E+\hbar\omega)dE, \qquad (1)$$

where apart from the standard physical meaning of e, m, c, ω and n (the electron charge, the electron mass, the speed of the light, the frequency and the refractive index) the quantity P is the energy independent optical matrix element, energy independent V$_{cell}$ (an analog to a primitive crystal cell) meaning that considered absorption is independent of the volume of localization, g$_i$ and g$_f$ are the densities of the initial (g$_i$) and final (g$_f$) state of the optical transition and ℏω is the photon energy [17]. Using: g$_i$(E) ~ g$_v$(E$_v$-E)$^{1/2}$ and g$_f$(E) ~ g$_c$(E-E$_c$)$^{1/2}$, from equation (1) follows for both the Tauc model and the Davis Mott model: α = B(ℏω – E$_g$)^2/ℏω. Within the Davis – Mott

model the slope (B) of the short wavelength absorption edge contains the information about the width of the localized states at the band edges. This approach means that the high density states below (E_v) and above (E_c) are considered where E_v and E_c correspond to the energy of the edge of valence and conduction states, respectively. For a more detailed definition, see [16 and 17]. Hence due to the high density states ($\alpha > 10^3 – 10^4$ cm^{-1}) only samples with a very small thickness can be used for the measurement of the optical transmission.
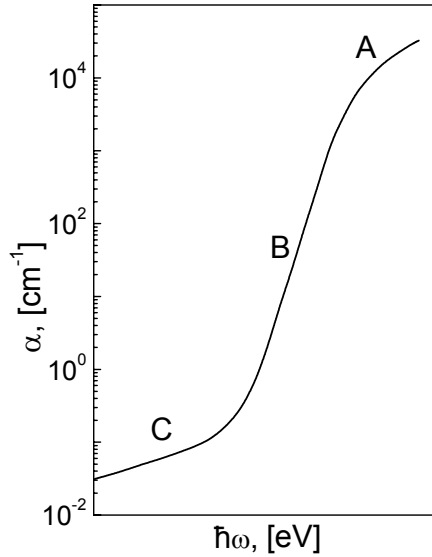

Fig. 1. Schematic spectral dependence of the absorption coefficient – the parts A,B,C of SWAE [17].

In part B, the exponential region, the absorption coefficient is expressed by the equation [17]:

$$\alpha = [2(\pi e)^2 \hbar f \, V_{cell} \, /mcn] \int g_{tail}(E_i) g_c(\hbar\omega - E_g + E_i) dE_i, \quad (2)$$

where f is the oscillator strength, E_i is the width of the localized tail state at the valence band having an exponential shape: $g_{tail}(E_i) = N exp(-E_i/E_t)/E_t$, where E_t is a certain constant and N is the concentration of the tail states. Hence one obtains: $\alpha \sim exp(\hbar\omega/E_e)$, the relation reminiscent of the Urbach type edge [18], where E_e reflects how steeply the exponential tail fails down into the gap. Since the density of states corresponding to E_i is much lower than the one responsible for the part A of $\alpha(\hbar\omega)$ dependence (Fig. 1), the thicker sample has to be used for the optical transmission measurements since in

the thin sample (d in the order of μm), the absorption associated with the tail states is too weak to be reliably observed.

If the multiple internal reflections are considered and the interference effects are averaged out or absent, also in the spectral region of SWAE, the optical transmission of the plan parallel sample plate is given by relation [19]:

$$T=[(1-R)^2 exp(-\alpha d)]/[1-R^2 exp(-2\alpha d)], \quad (3)$$

where T, R and d are the optical transmission, the reflectivity and the sample thickness, respectively. For the reader's convenience in Table 1 the values of T calculated using rel. (3) for $R_{(n=2)} = 0.147$ and for some α and d values to illustrate the crucial role of the sample thickness on the data relevance to the employing Tauc and /or Davis - Mott model are shown.

Table 1. The reflectivity for n=2, the absorption coefficient, the thickness and calculated values of the optical transmission, rel. (3).

$R_{(n=2)}$ [%]	α [cm^{-1}]	d [cm]	T [%]
14.7	10^4	3×10^{-4}	3.623
14.7	10^3	3×10^{-3}	3.623
14.7	10^3	3×10^{-2}	6.8×10^{-12}
14.7	10^2	3×10^{-2}	3.623

It is evident from Table 1 that one can hardly use the sample of the thickness of order 0.3 mm for a correct estimation of the optical band gap within the model of Tauc and /or Davis- Mott, whereas it can be used for the measurements in the B region of SWAE.

3. Experimental and calculated optical band gap values

The non-direct optical band gap values were determined using the Davis – Mott model [16]. Classical optical transmission on the bulk samples with the thickness varying in the region 0.5 – 4 μm prepared by a glass blowing was measured. The optical band gap values, see Table 2, were determined using the relation $(\alpha\hbar\omega)^{1/2} = B^{1/2}(\hbar\omega – E_g)$. For details regarding the samples preparation and the other experimental details see the references in the footnote to Table 2.

Table 2. The sample number and the chemical composition, experimental (E_g) and calculated ($E_{g,calc}$) optical band gap values.

Chemical composition	E_g [eV]	$E_{g,calc.}$ [eV]	Chemical composition	E_g [eV]	$E_{g,calc}$ [eV]
1.$(PbO)_{30}(ZnO)_{10}(P_2O_5)_{60}$	4.98	5.34	24.$(Bi_2O_3)_5(ZnO)_{15}(TeO_2)_{80}$	3.58	3.25
2.$(PbO)_{35}(ZnO)_{10}(P_2O_5)_{55}$	4.96	5.13	25.$(Bi_2O_3)_5(ZnO)_{25}(TeO_2)_{70}$	3.51	3.24
3.$(PbO)_{40}(ZnO)_{10}(P_2O_5)_{50}$	4.93	4.92	26.$(Bi_2O_3)_{10}(ZnO)_{15}(TeO_2)_{75}$	3.49	3.22
4.$(PbO)_{45}(ZnO)_{10}(P_2O_5)_{45}$	4.82	4.69	27.$(Bi_2O_3)_{10}(ZnO)_{25}(TeO_2)_{65}$	3.46	3.21
5.$(PbO)_{50}(ZnO)_{10}(P_2O_5)_{40}$	4.7	4.48	28.$(Li_2O)_{7.5}(TiO_2)_{7..5}(TeO_2)_{85}$	3.3	3.54
6.$(PbO)_{55}(ZnO)_{10}(P_2O_5)_{35}$	4.6	4.27	29.$(Li_2O)_{10}(TiO_2)_{10}(TeO_2)_{80}$	3.4	3.62
7.$(PbO)_{50}(P_2O_5)_{50}$	4.91	4.86	30.$(Li_2O)_{12..5}(TiO_2)_{12.5}(TeO_2)_{75}$	3.2	3.7
8.$(PbO)_{50}(ZnO)_5(P_2O_5)_{45}$	4.71	4.67	31.$(BaO)_{7.5}(TiO_2)_{7..5}(TeO_2)_{85}$	3.3	3.75
9.$(PbO)_{50}(ZnO)_{15}(P_2O_5)_{35}$	4.6	4.29	32.$(BaO)_{10}(TiO_2)_{10}(TeO_2)_{80}$	3.2	3.35
10.$(PbO)_{50}(ZnO)_{20}(P_2O_5)_{30}$	4.64	4.11	33.$(BaO)_{12..5}(TiO_2)_{12.5}(TeO_2)_{75}$	3.3	3.36
11.$(PbO)_{60}(P_2O_5)_{40}$	4.72	4.44	34.$(Bi_2O_3)_{10}(WO_3)_{20}(TeO_2)_{70}$	3.36	3.11
12.$(PbO)_{40}(ZnO)_{20}(P_2O_5)_{40}$	4.71	4.53	35.$(Bi_2O_3)_8(WO_3)_{23}(TeO_2)_{69}$	3.21	3.11
13.$(PbO)_{30}(ZnO)_{30}(P_2O_5)_{40}$	4.63	4.58	36.$(Bi_2O_3)_{10}(WO_3)_{30}(TeO_2)_{60}$	3.23	3.05
14.$(PbO)_{20}(ZnO)_{40}(P_2O_5)_{40}$	4.82	4.63	37.$(Bi_2O_3)_{10}(WO_3)_{35}(TeO_2)_{55}$	3.23	3.02
15.$(PbO)_{10}(ZnO)_{50}(P_2O_5)_{40}$	4.93	4.67	38.$(PbO)_{10}(WO_3)_{20}(TeO_2)_{70}$	3.26	3.12
16.$(ZnO)_{60}(P_2O_5)_{40}$	4.9	4.72	39.$(PbO)_{10}(WO_3)_{30}(TeO_2)_{60}$	3.27	3.27
17.$(PbO)_{15}(ZnO)_{15}(P_2O_5)_{70}$	5.39	5.78	40.$(PbO)_{14}(WO_3)_{28}(TeO_2)_{58}$	3.14	3.05
18.$(PbO)_{20}(ZnO)_{15}(P_2O_5)_{65}$	5.23	5.58	41.$(Nb_2O_5)_{10}(TeO_2)_{90}$	3.42	3.31
19.$(PbO)_{25}(ZnO)_{15}(P_2O_5)_{60}$	5.38	5.36	42.$(Nb_2O_5)_{20}(TeO_2)_{80}$	3.45	3.31
20.$(PbO)_{30}(ZnO)_{15}(P_2O_5)_{55}$	5.16	5.15	43.$(PbO)_{10}(Nb_2O_5)_{10}(TeO_2)_{80}$	3.45	3.25
21.$(PbO)_{35}(ZnO)_{15}(P_2O_5)_{50}$	4.95	4.94	44.$(PbO)_{10}(Nb_2O_5)_{20}(TeO_2)_{70}$	3.39	3.26
22.$(PbO)_{40}(ZnO)_{15}(P_2O_5)_{40}$	5.10	4.72	45.$(PbO)_{20}(Nb_2O_5)_{10}(TeO_2)_{70}$	3.51	3.19
23.$(PbO)_{45}(ZnO)_{15}(P_2O_5)_{40}$	4.85	4.51	46.$(PbO)_{20}(TeO_2)_{80}$	3.61	3.19

For more experimental details see: the samples 1-16 [22], the samples 17-23 [23], the samples 24-27 [3], the samples 28-33 [24], the samples 34-40 [4], the samples 41-46 [25].
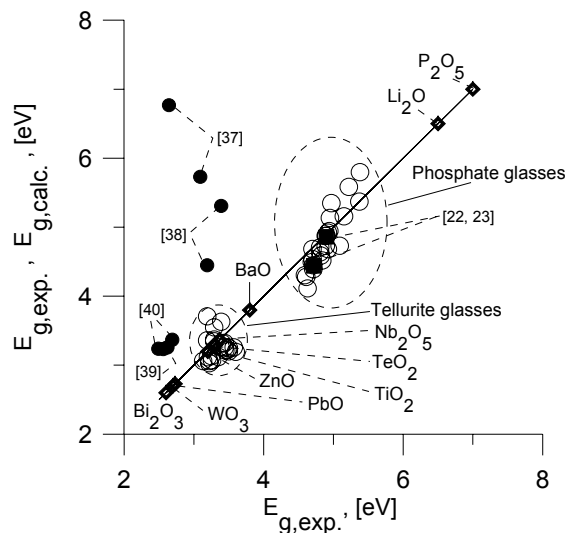

Fig. 2. The line – corresponds to our experimental versus our experimental band gap values and the experimental versus experimental band gap values of binary oxides (diamonds): $E_g(TeO_2) \approx 3.3$ eV [26], $E_g(P_2O_5) \approx 7eV$ is a tentative estimation of the lowest limit of the band gap based on the band gap values for the single crystals like $NaAlP_2O_7$, $KAlP_2O_7$, E_g at around 6 eV [27], and E_g for PO_3^{2-} molecule, $E_g \approx 7$-10 eV [28]. $E_g(ZnO) \approx 3.2$ eV [29], E_g (Bi_2O_3) ≈ 2.6 eV as an average E_g value from Refs. [30, 31], E_g (PbO) ≈ 2.7-2.8 eV [32], $E_g(BaO) \approx 3.9$ eV [33], $E_g(Li_2O) \approx 6.5$ eV [34], $E_g(WO_3) \approx 2.7$ eV [35], $E_g(Nb_2O_5) \approx 3.37$ eV [35], $E_g(TiO_2) \approx 3.3$ eV [36]. The open circles - calculated (rel.5) versus our experimental band gap values. The full circles calculated (rel. 5) versus experimental band gap values taken from Refs. [37 – 40] - examples of a typical reduction in the band gap values determined employing Tauc or Davis Mott model for the spectral region relevant to the Urbach like edge. It means that the absorption due the tail states was interpreted as the absorption corresponding to the transitions between $g_v \rightarrow g_c$ states. Black squares – our experimental values of $E_g = 4.91$ eV and 4.72 eV for $(PbO)_{0.5}(P_2O_5)_{0.5}$ and $(PbO)_{0.6}(P_2O_5)_{0.4}$, respectively. The numbers in square brackets correspond to the relevant references.

For some binary crystalline alloys the compositional trends in the band gap can be estimated using a simple alloying model [20]:

$$E_g(A_xB_{1-x}) = xE_{g,A} + (1-x)E_{g,B} \pm \gamma\, x(1-x), \qquad (4)$$

where x is the molar fraction of components A, B of the alloy, $E_{g,A}$ and $E_{g,B}$ are the band gaps of the components A, B and γ is the bowing parameter and it is a measure of the departure of the system from ideal behavior. Shimakawa [21] initially showed that rel. (4) can be used for calculation of the compositional trends in the band gap for various binary noncrystalline chalcogenide systems. Assuming in the first approximation that $\gamma = 0$ we used the relation (4) for the calculation of the optical band gap values of the ternary glasses examined in the form:

$$E_g(A_xB_yC_z) = xE_{g,A} + yE_{g,B} + zE_{g,C}, \qquad (5)$$

where A, B and C are the oxides forming the glass and x + y + z = 1. In Fig. 2 our experimental band gap values and the calculated band gap values versus the experimental band gap values are plotted.

From Fig. 2 and the data summarized in the Table 2 two facts are clear:
(i) The experimental band gap values are generally higher than the band gap values quoted in the relevant literature for similar and/or the same glasses. For instance, our experimental band gap values for $(PbO)_{0.5}(P_2O_5)_{0.5}$ and $(PbO)_{0.6}(P_2O_5)_{0.4}$ glasses are approximately 1.5 eV higher than the experimental band gap values determined for the glasses of the same or similar chemical composition: $E_g((PbO)_{0.6}(P_2O_5)_{0.4}) = 3.2$ eV and $E_g((PbO)_{0.4}(P_2O_5)_{0.6}) = 3.4$ eV [38]. The band gaps we determined for PbO-ZnO-P_2O_5 glasses vary from 4.6 eV for $(PbO)_{55}(ZnO)_{10}(P_2O_5)_{35}$ and $(PbO)_{50}(ZnO)_{15}(P_2O_5)_{35}$ to 5.39 eV for $(PbO)_{15}(ZnO)_{15}(P_2O_5)_{70}$. Similarly for TeO_2 based glasses we determined the band gap values by about 0.6 - 0.9 eV higher than those recently published. For the glasses $(Bi_2O_3)_{10}(WO_3)_{20}(TeO_2)_{70}$ and $(Bi_2O_3)_{10}(WO_3)_{30}(TeO_2)_{60}$ E_g was 2.67 eV and 2.5 eV [40], respectively, while we determined E_g of 3.36 eV and 3.2 eV, respectively. Similarly E_g was quoted 2.57 eV and 2.63 eV [39], respectively for the glasses $(Bi_2O_3)_{10}(ZnO)_{15}(TeO_2)_{75}$ and $(Bi_2O_3)_5(ZnO)_{15}(TeO_2)_{80}$, whereas we determined E_g of 3.49 eV and 3.58 eV, respectively. The reduction in the band gap values determined by application of the relation : $(\alpha\hbar\omega)^{1/2} = B^{1/2}(\hbar\omega - E_g)$ to the spectral region where it is valid: $\alpha \sim \exp(\hbar\omega/E_e)$ [17] reflects the fact that $B(\hbar\omega - E_g)^2/\hbar\omega \neq \alpha_0\exp(\hbar\omega/E_e)$ because at least: $g_v(E_v\text{-}E)^{1/2} \neq N\exp(\text{-}E_i/E_t)/E_t$, see equations (1, 2) and [17].

For the case where the samples with the thickness of order mm are only available and it is not possible to prepare the sample with the thickness of order μm for correct measurements of the optical absorption in the spectral region A ($\alpha = B\,(\hbar\omega - E_g)^2/\hbar\omega$), Fig. 1, we recommend estimating the optical band gap using the relation [41]:

$$\alpha = (10^3\ cm^{-1})\ \exp\left[(\hbar\omega - E_g^{03})/E_e\right], \qquad (6)$$

where $E_g \approx E_g^{03} = \hbar\omega_{(\alpha\ =\ 10^3\,cm\text{-}1)}$ is the energy for α extrapolated to $\alpha = 10^3\ cm^{-1}$. Using this relation we estimated, from Fig. 5 at [40], E_g^{03} the values for glasses $(Bi_2O_3)_{10}(WO_3)_{20}(TeO_2)_{70}$ and $(Bi_2O_3)_{10}(WO_3)_{30}(TeO_2)_{60}$ at around 3.4 eV which is quite comparable with our E_g values of 3.36 eV and 3.2 eV, respectively.

(ii) The difference (dE_g) between the experimental and calculated band gap values is the highest for the glass: $(PbO)_{50}(ZnO)_{20}(P_2O_5)_{30}$, $dE_g = 0.53$ eV, while for the other glasses applies $-0.4 < dE_g$ [eV] < 0.53 with the average value $|dE_g| = 0.28$ eV. This seems to be a quite reasonable value which is less than 9 % of the band gaps of TeO_2 based glasses and less than 6 % of the band gaps of P_2O_5 based glasses, see Table 2.

The simple alloying model ($\gamma = 0$) we used for the calculation of the optical band gap values reflects the fact that an interaction between the binary components of a glass does not lead to significant structural changes. Generally a certain interaction between the binary components might be present and which probably results in an increase in the band gap. A typical example is the case of $Ge_{1-x}S_x$ glasses where a well pronounced local maximum for $E_g(x = 0.66)$ reflects an ordering and formation of GeS_2 compound [42]. However, the broadening of the valence and conduction bands due to an increase in disorder can compensate for the band gap increase and hence the overall bowing parameter is close to zero. This could be the reason why a very simple alloying model provides a reasonable estimate of the optical band gap for the considered glasses.

4. Conclusion

In this paper we recapitulated certain facts and experimental conditions which should be considered if the Tauc model and/or the Davis-Mott model is to be used for determination of the optical band gap in glasses. It was emphasized that it is not possible to interpret absorption associated with the Urbach –like edge as absorption relevant to a non-direct band gap. For 46 heavy metal oxide glasses the optical band gap values determined using the Davis-Mott model were summarized. These band gap values are at least approximately 30% higher than the band gap values claimed in the literature for the same or similar glasses.

References

[1] S. Bale, S. Rahman, J. Non-Cryst. Solids **355**, 2127 (2009).

[2] J. Schwarz, H. Ticha, L. Tichy, Mat. Letters **61**, 529 (2007).

[3] J. Ozdanova, H. Ticha, L. Tichy, J. Non-Cryst. Solids **353,** 2799 (2007).

[4] J. Ozdanova, H. Ticha, L. Tichy, J. Non-Cryst. Solids **355,** 2218 (2009).

[5] T. S. Moss, Proc. Phys. Soc**. B63**, 167 (1950).

[6] N. M. Ravindra, V. K. Srivastava, Infrared Phys. **19**, 603 (1979).

[7] P. Herve, L. K. J. VanDamme, Infrared Phys. Technol. **35**, 609 (1994).

[8] R. R. Reddy, Y. N. Ahammed, K. R. Gopal, D. V. Raghuram, Opt. Mater. **10**, 95 (1998).

[9] N. L. Boling, A. J. Glass, A. Owyoung, IEEE J. Quantum Electron. **QE-14**, 601 (1978).

[10] M. Sheik-Bahae, D. J. Hagan, E. W. Stryland, Phys. Rev. Letters **65**, 96 (1990).

[11] H. E. Lines, Phys. Rev. B **41**, 3383 (1990).

[12] H. Ticha, L. Tichy, J. Optoelectron. Adv. Mater., **4**, 381 (2002).

[13] Ke. Tanaka, J. Phys. Chem. Solids **68**, 896 (2007).

[14] O. Sanz, E. Haro-Poniatowski, J. Gonyalo, J. M. F. Navarro, J. Non-Cryst. Solids **352**, 761 (2006).

[15] J. Tauc, A. Abraham, L. Pajasova, R. Grigorovici, A. Vancu, Proceedings of the International Conference Physics of Non-Crystalline Solids, North-Holland Amsterdam, 1965, p. 6069.

[16] E. A. Davis, N. F. Mott, Philos. Mag. **22**, 903 (1970).

[17] J. Tauc, Optical Properties of Amorphous Semiconductors in: Amorphous and Liquid Semiconductors, J.Tauc (Ed.) Plenum, London and New York, 1974.

[18] F. Urbach, Phys. Rev. **92**, 1324 (1953).

[19] J. I. Pankove, Optical Processes in Semiconductors, Prentice-Hall, Inc., Englewood Cliffs, New Jersey, 1971.

[20] J. C. Phillips, Bonds and Bands in Semiconductors, Academic Press, New York and London, 1973.

[21] K. Shimakawa, J. Non-Cryst. Solids **43**, 229 (1981).

[22] H. Ticha, J. Schwarz, L. Tichy, R. Mertens J., Optoelectron. Adv. Mater., **6**(3), 747 (2004).

[23] K. Kotkova, H. Ticha, L. Tichy, Optoelectron. Adv. Mater.-Rapid Commun. **1**(1), 36 (2007).

[24] J. Ozdanova, H. Ticha, L. Tichy, Adv. Mat. Res. **39-40**, 185 (2008).

[25] J. Ozdanova, H. Ticha, L. Tichy, Opt. Mat. **32**, 950 (2010).

[26] K. Terashima, Sae-Hoob Kim, T.Yoku, J. Amer. Ceram. Soc. **789**, 169 (1995).

[27] A. Hizhnyi, A. Oliynyk, O. Gomenyuk, S.G. Nedilko, P. Nagornyi, R. Bojko, V. Bojko, Opt. Mat. **30**, 687 (2008).

[28] S. Saito, K. Wada, R. Onaka, J. Phys. Soc. Japan **37**, 711 (1974).

[29] Ch. Y. Tsai, Ch. W. Wu, Ch. M. Lei, F. S. Chen, Ch. K. Lin, Thin Solid Film **519**, 1516 (2010).

[30] J. M. Carlson, Bo. Hellsing, H. S. Domongos, P. D. Bristowe, Phys. Rev. B **65**, 2005122 (2002).

[31] H. T. Fan, S. S. Pan, X. M. Teng, C. Ye, G. H. Li, J. Phys. D: Appl. Phys. **39**, 1939 (2006).

[32] H. J. Terpstra, R. A. deGroot, C. Haas, Phys. Rev. B**52**, 11690 (1995).

[33] T. Lv, D. Chen, M. Huang, J. Appl. Phys. **100**, 086103 (2006).

[34] M. Moakafi, R. Khenata, A. Bouhemadou, H. Khachai, B. Amrani, D. Rached, M. Rérat, Eur. Phys. J. B **64**, 35 (2008).

[35] W. H. Strehlow, E. L. Cook, J. Phys. Chem. Ref. Data **2**, 163 (1979).

[36] R. Ayouchi, C. Casteleiro, R. Schwarz, J. R. Barrado, F. Martín, physica status solidi (c) **7**, 933 (2010).

[37] L. M. Sharaf El-Deen, M. S. Al Salhi, M. M. Elkholy, J. Non-Cryst. Solids **354**, 3762 (2008).

[38] V. Sudarsan, S. K. Kulshreshtha, J. Non-Cyrst. Solids **286**, 99 (2001).

[39] E. Yousef, M. Hotzel, C. Rüssel, J. Non-Cryst. Solids **353**, 333 (2007).

[40] T. Y. Chen, Q. Nie, T. Xu, S. Dai, X. Wang, X. Shen, J. Non-Cryst. Solids **354**, 3468 (2008).

[41] M. Munzar, C. Koughia, D. Tonchev, K. Maeda, T. Ikari, C. Haugen, R. Decorby, J. N. McMullin, S. O. Kasap, Opt. Mat. **28**, 225 (2006). 5.

[42] L. Tichy, A. Triska, M. Frumar, H. Ticha, J. Klikorka, J. Non-Cryst. Solids **50**, 371 (1982).

_____

*Corresponding author: ladislav.tichy@upce.cz